Theoretical and Applied Climatology
https://doi.org/10.1007/s00704-023-04476-3

RESEARCH

# Spatial analysis and optimization of raingauge stations network in urban catchment using Weather Research and Forecasting model

**Rasoul Sarvestan[1] · Mokhtar Karami[1] · Reza Javidi Sabbaghian[2]**

Received: 1 January 2023 / Accepted: 6 May 2023


**Abstract**
Hydrological modelling, especially in urban catchments, relies heavily on accurate rainfall data collection. Therefore, rainfall estimation and establishing a network of raingauge stations is essential, especially for regions with a limited number of stations. To simulate rainfall, the Weather Research and Forecasting (WRF) model was used in this study based on the six schemes including Lin, WSM3, WSM5, WSM6, WDM5, and WDM6. Furthermore, optimal spatial design of raingauge networks has been achieved using geostatistical and deterministic interpolation methods of Radial Basis Function (RBF), Local Polynomial Interpolation (LPI), Co-Kriging (COK), Inverse Distance Weighting (IDW), Global Polynomial Interpolation (GPI), and Empirical Bayesian Kriging (EBK). Hence, the error reduction in estimating rainfall on non-station points was considered as an indicator to determine the optimal location of stations. This study was conducted in the Sabzevar urban catchment in northeastern Iran, which faces significant flood damages in a few raingauge stations. Initially, the 24-h rainfall data on the five events (from winter to spring 2019 ~ 2020), covering all types of rainfall associated with the seasons, were selected for analysis. The results revealed that among the WRF model schemes, the Lin was chosen as the most desirable scheme to simulate the rainfall in the catchment. A positive verification criterion result between 0.65 and 1 also shows that rainfall values can be estimated efficiently by this scheme over a distance of 18.85 km from the observational raingauge station. Furthermore, based on the interpolation results, the RBF method with the highest $R^2$ (98%) was the most accurate method for the optimal location of the stations in non-station points, i.e., the WRF model outputs with observational stations. Overall, it can be concluded that using the WRF meteorological model combined with the RBF interpolation method could be appropriate for simulating the rainfall, designing the raingauge stations, and forecasting highly accurate 24-h rainfall, especially for the urban catchment without stations. The proposed approach used in this study is also recommended to develop the optimal design of raingauge networks of non-station points in large catchments.

## 1 Introduction

Extreme rainfall events cause casualties, infrastructure damages, and economic and social damages around the world every year (Handmer et al. 2012; O'Gorman 2015; Hu et al. 2020; de Bodas Terassi et al. 2020). Potential meteorological knowledge (precipitation) of these extreme events is essential for the implementation of many programs, including risk management, socioeconomic development, and planning at global, regional, and local levels (Hu et al. 2020). Understanding the trends of climatic variables and severe weather conditions, as well as their effects on water resources and crisis management, is becoming increasingly critical (Jones et al. 2003; Steduto et al. 2009; Xavier et al. 2016). However, interpreting these climatic variables is difficult due to the highly variable nature of meteorological processes, land, geography, and the difficulty in establishing station representative networks (Shimizu 1993; Kedem et al. 1990; Yoo et al. 2008; Huang et al. 2022). Obtaining accurate weather data requires information about the density and location of meteorological stations (Ashraf et al. 1997). Despite their high accuracy, in most cases, raingauge networks are too

✉ Mokhtar Karami
M.Karami@hsu.ac.ir; M.Karami08@Yahoo.co.uk

Rasoul Sarvestan
r.sarvestan@gmail.com

Reza Javidi Sabbaghian
r.javidi.s@hsu.ac.ir; rezajs.civil.eng@gmail.com

[1] Department of Climatology, Faculty of Geography & Environmental Sciences, Hakim Sabzevari University, Sabzevar, Iran

[2] Department of Civil Engineering, Faculty of Engineering, Hakim Sabzevari University, Sabzevar, Iran

Published online: 27 May 2023

sparsely distributed to accurately measure the spatial and temporal variations of precipitation systems (Villarini et al. 2008). These networks are often used to produce estimates of average precipitation in the area or spot precipitation at specific locations. The accuracy of these tools depends on the total number and location of the network (Cheng et al. 2008). The show still has limitations, even if raingauges provide accurate rain measurements. There are very few (or none) Raingauge networks on most of the planet to capture the variety of rainfall systems over time and space (Villarini et al. 2008). Hence, information required for forecasting — flood warnings, hydraulic structure designs, water scarcity, and regional droughts are all greatly affected by these uncertainties (Bayat et al. 2019). Therefore, it is better to design an appropriate network of the meteorological dataset with a minimum number of stations to provide reliable data with both regional average and Spatio-temporal diversity (Xu et al. 2015). In addition to being reliable, these data networks must accurately record the region's average rainfall. In other words, it must be sufficiently accurate to reduce the standard error of rainfall in the region to a statistically insignificant level (Bayat et al. 2019). Although radars are subject to uncertainties and biases due to limitations in displaying basic processes as well as poor parameter estimates and inaccuracies in gages, they are widely used for estimating precipitation and planning station networks in areas with no stations (Kedem et al. 1990; Shimizu 1993). This is especially true in semi-mountainous and plain catchments due to the blockage of rays (Morin et al. 2003, 2005) by mountains and plains (Young et al. 1999; Smith et al. 1996; Volkmann et al. 2010). However, it is more difficult to estimate the depth and intensity of storms than on flat land. Various methods have been used around the world to estimate rainfall and design rainfall grids (Table 1). For example, Tekleyohannes et al. (2021) used a multi-criteria decision analysis (MCDA) in combination with kriging and Entropy methods in the Tekeze River basin, a trans-boundary river in the northwestern part of Ethiopia, to determine the desired number of stations. The results showed that the combined use of MCDA, kriging, and Entropy methods is useful for optimizing the spatial distribution and th number of raingauge stations in an area. Shafiei et al. (2014) evaluated rainfall accuracy using Geographic Information System (GIS) to operate and strengthen raingauge networks in a large catchment in Iran. The results showed that out of 33 raingauge stations, only 21 stations had a significant effect on rainfall. A summary of the most important recent studies in the regions of the world can be found in Table 1.

Recently, most studies have used entropy and kriging methods to simulate rainfall and design raingauge networks in large catchments. In addition, remote sensing data have been used to distribute raingauge stations. However, these data sets are widely associated with uncertainties in rainfall estimation because of spatial/temporal variability and non-uniform raingauge distribution in small urban catchments. Therefore, the estimate of average rainfall in urban catchments depend on the accuracy of data in various raingauge networks, which play an important role in many hydrological modelling applications. Hence, this study aimed to address these limitations as much as possible using dynamic meteorological WRF downscaling models at the regional and micro scales. However, the WRF model used the appropriate interpolation methods in addition to the precipitation simulation to obtain the rainfall values in the points that do not have a synoptic or Raingauge station. Accordingly, an optimal spatial design of a raingauge station network with appropriate accuracy has been implemented in the region.

## 2 Methods and materials

### 2.1 Study area

This study was conducted in the city of Sabzevar in Khorasan Razavi province in northeastern Iran ("36° 9′ 7" and 36° 22′ 30" N, 57° 37′ 30" and 57° 46′ 10" E, and 970 m above the sea level) (Khorasan Razavi Census, 2006). The predominant climatic condition of this region is classified in the semi-arid type, estimated based on the De Martonne classification method. Its average annual precipitation is 206 mm and the maximum rainfall has been reported as about 30 mm/day (Amirahmadi et al. 2012; Meteorological Organization 2019). Figure 1 depicts the geographical location of the study area of Sabzevar urban catchment, where the position of the synoptic station has been specified. Furthermore, its observational data has been used for the WRF model simulation.

To conduct this research, two types of data have been used including observational data (from the synoptic station), and the Global Forecast System (GFS) data.

The observational data from the synoptic stations:

This type of data are used for the events shown in Fig. 2, have been provided from the National Meteorological Organization (Sabzevar synoptic station), which these events actually cover all the rainfall in the catchment. According to the purpose of the research (evaluation of the network of raingauge stations for areas that do not have stations or have limitation of the number of stations) and also the absence of a raingauge station for the study area, this station has been used.

The Global Forecast System (GFS) data:

For the forecasting process, the Global Forecast System (GFS) data are required. According to the study events, these data are downloaded since the previous day (24 h ago, at 00 GMT) and analyzed based on the WRF meteorological model. In this research, according to the scope of the study

**Table 1** Summary of the literature review of the recent studies in various regions of the world

| Author | Description | Model | Case study |
|---|---|---|---|
| Rossi et al. (2017) | There is a statistical difference between gauge stations and satellite-based products, as well as a difference in the rainfall events derived from these two sources. As a result, satellite rainfall cannot be directly compared with ground data, and local considerations of morpho-climatological factors are necessary | VRF[a], TRMM[b] | Italy |
| Cecinati et al. (2018) | The case study and synthetic experiments show that accounting for measurement uncertainty in raingauge interpolation generally improves rainfall estimates, provided the density of raingages is sufficient | Kriging | Dommel catchment, the Netherlands |
| Islam (2018) | The results showed that all six satellite products used to collect rainfall data are good at detecting precipitation but are poor at estimating it | PERSIANN[c], CMORPH[d], IMERG[e], IMERG-GC[f], GSMaP[g], GSMaP-GC[h] | Bangladesh |
| Shirali et al. (2020) | Short-term meteorological forecasting models were used to forecast floods. The results showed that the WRF model scheme was more accurate than the SVM and ANN models | WRF, ANN[i], SVM[j] | Southwest of Iran |
| El Afandi and Morsy (2020) | Used to forecast heavy rainfall similar to Sinai<br>These results showed that the WRF model performed more accurately in forecasting the short-term precipitation, and rainfalls that caused floods in this area | WRF | Sinai Peninsula |
| Khansalari et al. (2021) | As seen from the rainfall simulation observed from this event in the region, the Grell-Devenyi scheme is the superior configuration for forecasting the output simulation | WRF | Northern Iran |
| Mu et al. (2021) | In the dry season, CHIRP and CHIRPS underestimate rainfall, while in the wet season, they overestimate it. dnCHIRPS differs more from CHIRPS, and dnCHIRPS differs less from monthly rainfall | CHIRP[k], CHIRPS[l], dnCHIRPS[m] | the state of Rondônia in the Brazilian Amazon |

[a]Verifica Rischio Frana

[b]Tropical Rainfall Measuring Mission

[c]Precipitation Estimation from Remotely Sensed Information using Artificial Neural Networks

[d]Climate Prediction Centre (CPC) Morphing Technique

[e]Integrated Multi-satellite Retrievals for Global Precipitation Measurement

[f]Integrated Multi-satellite Retrievals for Global Precipitation Measurement gauge-calibrated

[g]Global Satellite Mapping of Precipitation

[h]Global Satellite Mapping of Precipitation gauge-calibrated

[i]Artificial Neural Network

[j]Support Vector Machines

[k]Climate Hazards Group Infrared Precipitation

[l]Climate Hazards Group InfraRed Precipitation with Station data

[m]dense rain gauge network Climate Hazards Group InfraRed Precipitation with Station data

area, a raingauge station is designed and created every 9 km (the output of the model is 9 km).

## 2.2 The proposed methodology and the research steps

Initially, the data from the only synoptic station in the city were analyzed, derived from the five selected rainfall events, to determine the amount of precipitation and the optimal location of the stations in the Sabzevar catchment. Events were selected from the rainy seasons, with all low, medium, and heavy precipitation considered representative of the study area. To obtain the most desirable forecast for the precipitation events in the urban catchment, the events were then simulated based on the six schemes of the WRF meteorological model. The rainfall simulations were compared with observational data from the study area stations using six schemas: WSM3, WSM5, WSM6 (Hong and Lim 2006; Hong et al. 2004; Naing 2021), WDM5 (Wang et al. 2011; Mahala et al. 2021), WDM6 (Guo et al. 2019; Hong et al. 2010), and Lin (Cao et al. 2021). Each of these schemas analyzed the microphysical schemes of the study area.

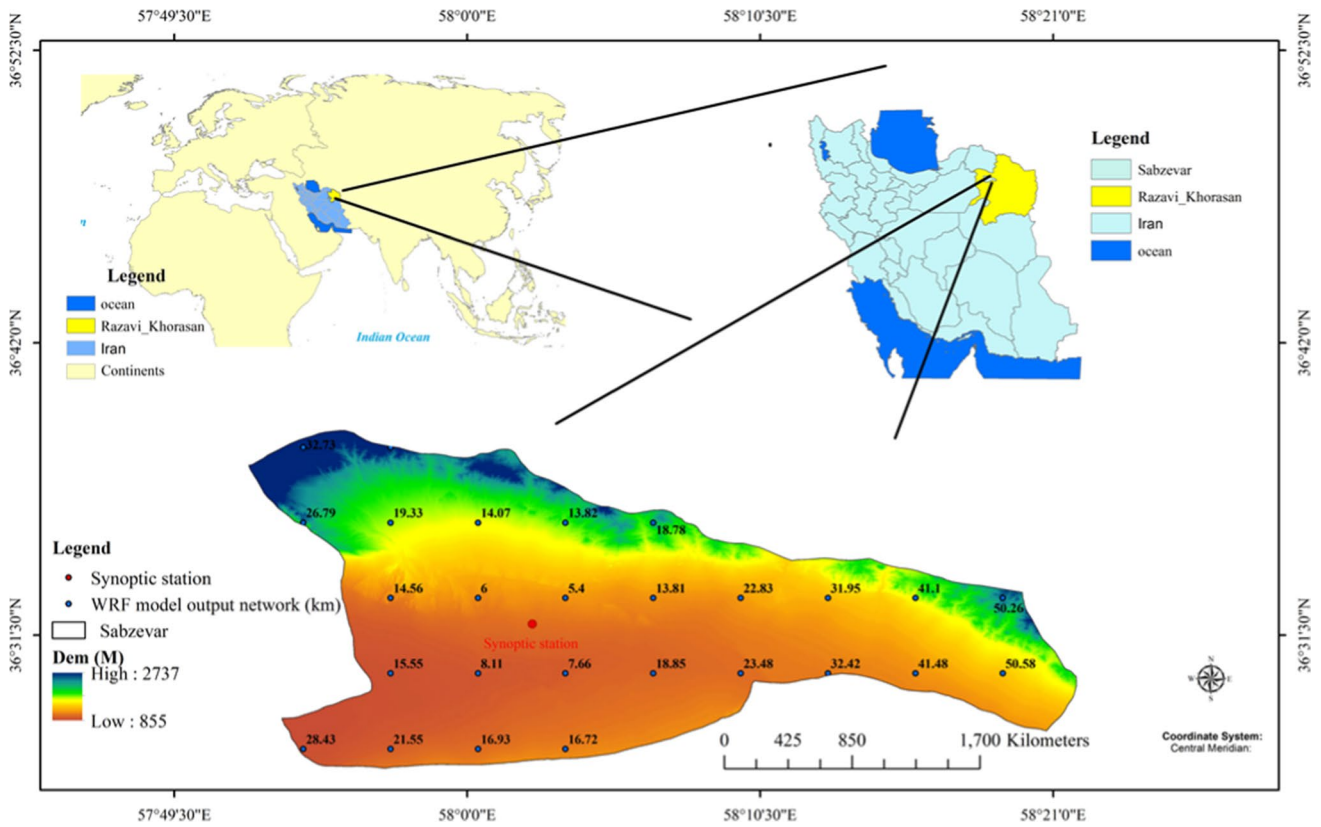


**Fig. 1** The geographical location for the study area of Sabzevar urban catchment in Khorasan Razavi province in Iran

It was then determined which schematic representation forecasted rainfall most accurately for each climate type. The reliability and accuracy of the simulation results were evaluated by the six verification criteria, which have been presented in Table 2. Accordingly, the verification criteria were used and the most desirable scheme was determined for the forecast process in the Sabzevar urban catchment. Furthermore, to determine the optimal location for the raingauge station network in the regions with no stations, the outputs of the WRF meteorological model have been used. These results included a 27 raingauge station network with a distance varies between 5.4 and 50.58 km from the observational station based on the five geostatistical and deterministic interpolation methods.

### 2.2.1 Interpolation methods

**Geostatistical interpolation methods** Geostatistical intermediation methods using spatial correlation of observations provide a continuous map via point data (Aalto et al., 2013). Half-variability is one of the most important tools for detecting and patterning spatial correlations between function observations (Goovaerts, 1997).

$$(h) = \frac{1}{2N(h)} \sum_{i=1}^{N(h)} \left[ Z\left(u_i + h\right) - Z(u_i) \right]^2 \quad (1)$$

where $(Y\,(h))$ is half the experimental variance, and $N\,(h)$ is the number of pairs of observations that are at h distance from each other. $Z\,(u_i)$ and $Z\,(u_i + h)$ are the observed values, which are variable at points $u_i$ and $u_i + h$, respectively. The geostatistical methods used in this study include COK and EBK, briefly discussed below.

1. Co-kriging method (COK)

This method is a type of multivariate co-kriging in which auxiliary information (based on the correlation between the main and auxiliary variables) is used for better estimation. Co-kriging estimator can be calculated from the equation (Isaaks and Srivastava, 1989).

$$Z_{COK}\,(u) = \sum_{i=1}^{n(u)} {}_i{}^{COK}.Z\left(u_i\right) + \sum_{j=1}^{m(n)} W_j^{COK}.e(u_j) \quad (2)$$

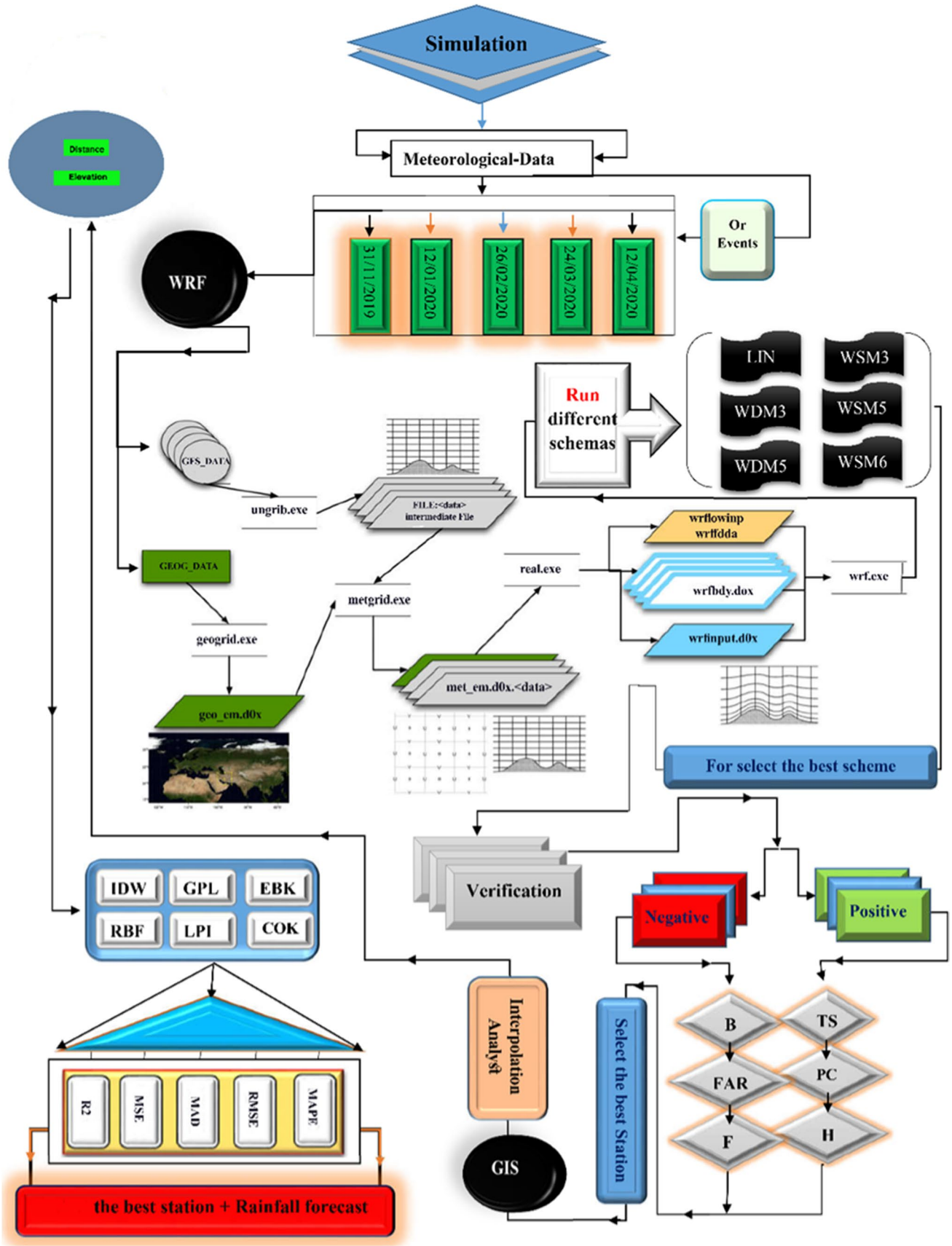


**Fig. 2** The proposed flow diagram for optimal location of the raingauge stations and rainfall forecast

**Table 2** The verification criteria and the relevant equations for evaluating the accuracy of the WRF model

| Type of criteria | Verification criterion | Verification equation | Acceptable value |
|---|---|---|---|
| Negative | Relative Bias (B) | $B = \frac{a+b}{a+c}$ | 1 |
| | False Alarm Ratio (FAR) | $\mathrm{FAR} = \frac{b}{a+b}$ | 0 |
| | False Alarm Rate (F) | $F = \frac{b}{b+d}$ | 0 |
| Positive | Proportion Correct (PC) | $\mathrm{PC} = \frac{a+b}{n}$ | 1 |
| | Threat Score (TS) | $\mathrm{TS} = \frac{a}{a+b+c}$ | 1 |
| | Hit Rate (H) | $H = \mathrm{POD} = \frac{a}{a+c}$ | 1 |

where $i$ and $w_j$ are the weights attributed to the observational values of the main and auxiliary variables at the point's $u_i$ and $u_j$, respectively.

2. Empirical Bayesian Kriging (EBK)

EBK is a geostatistical interpolation method that automates the most difficult aspects of building a valid kriging model. Although in other kriging methods, the parameters are manually adjusted to get accurate results, EBK automatically simulates and calculates these parameters through a process ((Esri, 2018 h).

**Deterministic methods for spatial interpolation** The definitive mediation methods used in this research include IDW, GPI, LPI, and RBF methods, which were briefly described below.

1. Inverse distance weighting (IDW)

The Kriging estimator is the main estimation relation in this method. However, the weights are determined solely by comparing the distances between known points and unknown points, without considering the distribution of the points around the estimated point (Deliri et al. 2009).

$$i = \frac{\frac{1}{d_i}}{\sum_{i=1}^{n} \frac{1}{d_i}} \tag{3}$$

where $d_i$ *i-th* is the distance of *i-th*, the observed point to the estimated point, the weighting power of the distance, and n is the number of adjacent points. Weights decrease as the distance between the known and unknown points increases.

2. Radial Basis Function (RBF)

In this method, the fitted surface should be placed from all the measured points. The values estimated using this method are based on mathematical functions that smooth the surface by reducing its overall curvature. The mathematical method of radius-axis functions is generally expressed in the equation (Zandi et al. 2011). Where $\|.\|$ expresses the length of the vector, x and y are the spatial variables, $(x_i, y_i)$ is the spatial coordinate, the spatial coordinate of the i-th observation point is the index $Z_i$ and $E$ is a RBF.$a_i, b_0, b_1, b_2$ are the coefficients that must be determined to specify the function explicitly.

The difference between the various RBF methods is how the functions are defined in the equation above.

$$f(x,y) = \sum_{i=1}^{n} a_i E\left(x - x_i, y - y_i\right) + b + b_1 x + b_2 y \tag{4}$$

3. Global Polynomial Interpolation (GPI)

GPI uses a mathematical function to fit a smooth surface to the sample points. The GPI surface changes gradually from region to region over the studied area and captures the global trend in the data. Unlike IDW, GPI calculates forecasts using the entire data set rather than measured points within neighborhoods. A first-order GPI fits a flat plane; a second-order GPI fits a surface, allowing for one bend; a third-order GPI allows for two bends, and so forth (Esri, 2018). However, a single global polynomial can hardly fit a surface with a varying shape. Thus, multiple polynomial planes are desired to better represent the surface.

4. Local Polynomial Interpolation (LPI)

Unlike GPI, LPI fits the local polynomial using points only within the specified neighborhood instead of all the data. Then the neighborhoods can overlap, and the surface value at the center of the neighborhood is estimated as the forecasted value. GPI is useful for detecting long-range trends in the dataset, while LPI can produce surfaces that capture short-range variation (Wang et al., 2014). Finally, to evaluate the accuracy of the interpolation methods, we used the five verification indices shown in Table 3. Figure 2 represents the proposed rainfall simulation flowchart, the optimal

**Table 3** The verification indices and the relevant equations for evaluating the accuracy of interpolation methods

| Verification index | Verification equation | Acceptable value |
|---|---|---|
| R-squared ($R^2$) | $R^2 = 1 - \frac{\text{First Sum of Errors}}{\text{Second Sum of Errors}}$ | 1 |
| Mean absolute percent error (MAPE) | $\text{MAPE} = \frac{100 \sum_{i=1}^{n} \left\lvert \frac{Y_i - \hat{Y}_i}{Y_i} \right\rvert}{n}$ | 0 |
| Mean absolute deviation (MAD) | $\text{MAD} = \sum_{i=1}^{n} \left\lvert \frac{Y_i - \hat{Y}_i}{n} \right\rvert$ | 0 |
| Root mean square error (RMSE) | $\text{RMSE} = \sqrt{\text{MSE}}$ | 0 |
| Mean square error (MSE) | $\text{MSE} = \frac{1}{n} \sum_{i=1}^{n} (Y_i - \hat{Y}_i)^2$ | 0 |

rain gage station location, and the rainfall forecast process based on the WRF model simulation and interpolation steps.

where $n$ is the total number of the observational events; $a$ is the number of times that the phenomenon occurs and its occurrence is forecasted, $b$ is the number of times that the phenomenon does not occur but its occurrence is forecasted, $c$ is the number of times that the phenomenon occurs but its occurrence is not forecasted, and $d$ is the number of times that the phenomenon does not occur and its occurrence is not forecasted. To make a good forecast, the a and b values need to be large, while the c and d values should be small.

Where $n$ is the number of the observational data and the total output values of the WRF meteorological model. $Y_i$ is the *ith* observational value of rainfall and $\hat{Y}_i$ is the *ith* simulated value of rainfall determined by the geostatistical methods.

## 3 Results and discussion

The reliability of the WRF modelling depends on the comparison between the observational and simulated rainfall values. Accordingly, the relevant difference between the observational and simulated values indicates the accuracy of the model but is used as a true test criterion for determining accuracy percentages and multipliers. According to Fig. 1, the Sabzevar synoptic station is applied as the observational station for the WRF modeling process. Subsequently, the rainfall values were estimated based on the WRF model schemes and compared with the data of the observational station for the five selected events. The scheme with the lowest difference between the calculated rainfall values and the observational data was selected as the most desirable scheme to simulate the rainfall. Figure 3 depicts the differences between the simulated rainfall estimated by the six WRF schemes and the observational data based on the several distances in the generated raingauges network from the synoptic station for the five events. Figure 3 a shows that on 11/31/2019, there is the smallest difference in precipitation between the WSM5 scheme results and the observed data (-1.44 mm), while the largest difference was associated with the WSM3 scheme (-2.66 mm). Regarding Fig. 3 b, the WSM6 scheme has the lowest precipitation difference for the 12/01/2020 event (2.44 mm), while the highest difference is associated with the WDM6 scheme (3.40 mm). Furthermore, Figs. 3c, 3d, and 3e illustrate that the Lin scheme has the smallest difference between precipitation and observed data for the events on 02/26/2020, 03/24/2020, and 04/12/2020 with the differences of 0.63 mm, 2.63 mm, and -12.12 mm, respectively. Also, the highest differences are associated with the WSM6, WSM3, and WDM6 schemes (1.36 mm, -5.46 mm, and 12.33 mm), respectively. As for heavy rainfall events (03/24/2020 and 04/12/2020), the Lin microphysical scheme showed higher accuracy for estimating the rainfall in the urban catchment. Based on the Lin scheme results for the above events, whose observed precipitation amounts are 36 mm and 28 mm, respectively, the rainfall differences were set to zero at distances less than 10 km from the synoptic station. If the distance was less than 10 km, the difference in the amount of precipitation was zero. Generally, the Lin scheme was accurate up to a distance of 18 km. It seems reasonable to choose a station up to this distance if its difference is either zero or 1–2 mm. Based on the results of the WRF model for the raingauges network, the precipitation differences associated with the Lin scheme were set to zero at some distances of the generated raingauges network, such as 5.4 km, 6 km, 7 km, and 8 km, for the events on 02/26/2020, 03/24/2020, and 04/12/2020. Indeed, for three of the five selected rainfall events, the Lin scheme has less rainfall difference from the observational station data.

Consequently, it can be argued that the Lin microphysical scheme can simulate and scale the rainfall values with a lower difference at both levels of the observational station and the 27 rain grids resulting from the WRF model output, especially up to a distance of 18.85 km from the observation station.

### 3.1 Verification criteria results

According to the verification stage, Fig. 4 demonstrates the negative and positive verification criteria related to each of the six WRF schemes for the study area based on the distances in the generated raingauges network from the

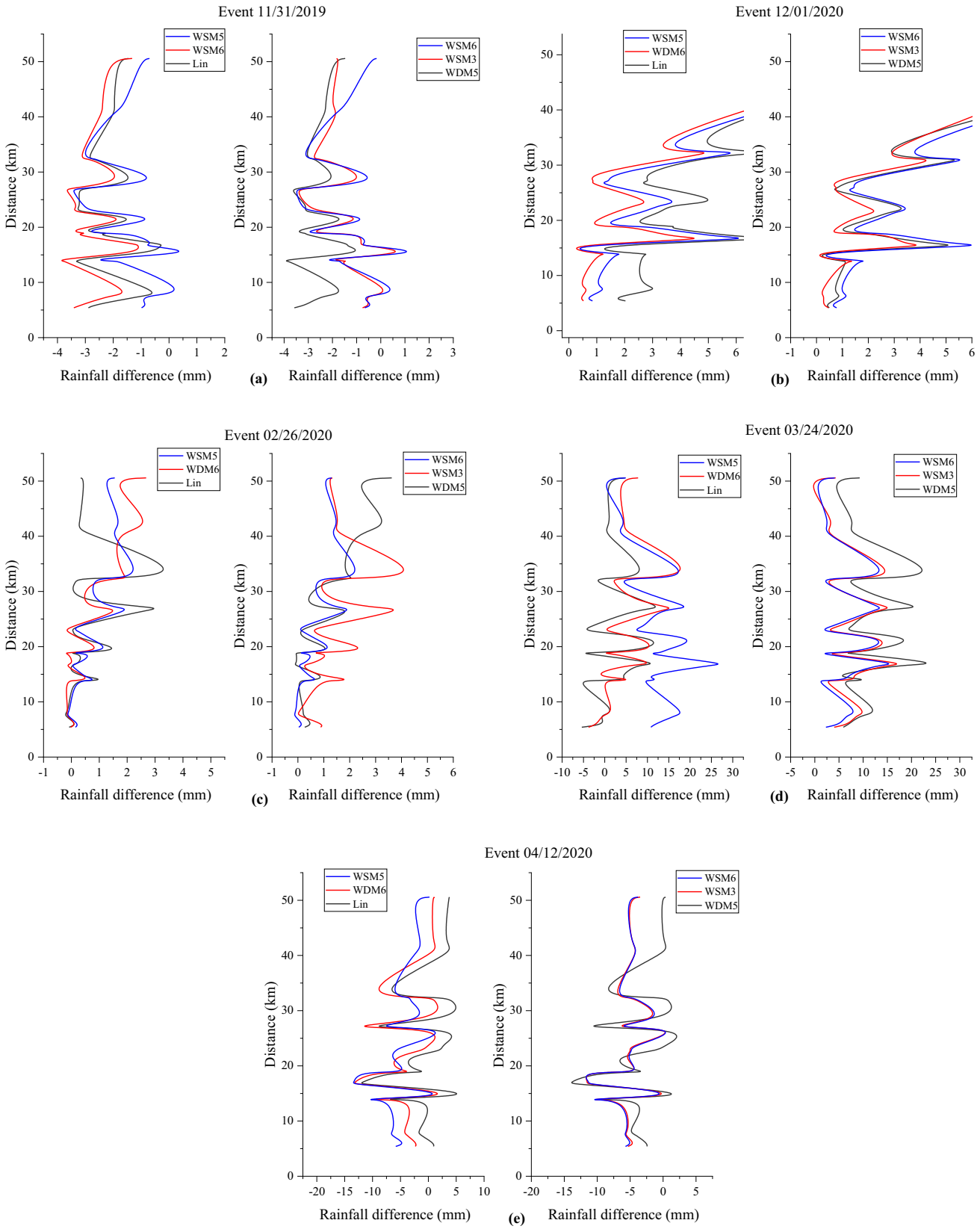


**Fig. 3** The differences between the simulated rainfall estimated by the six WRF schemes and the observational data based on the several distances from the synoptic station for the five events

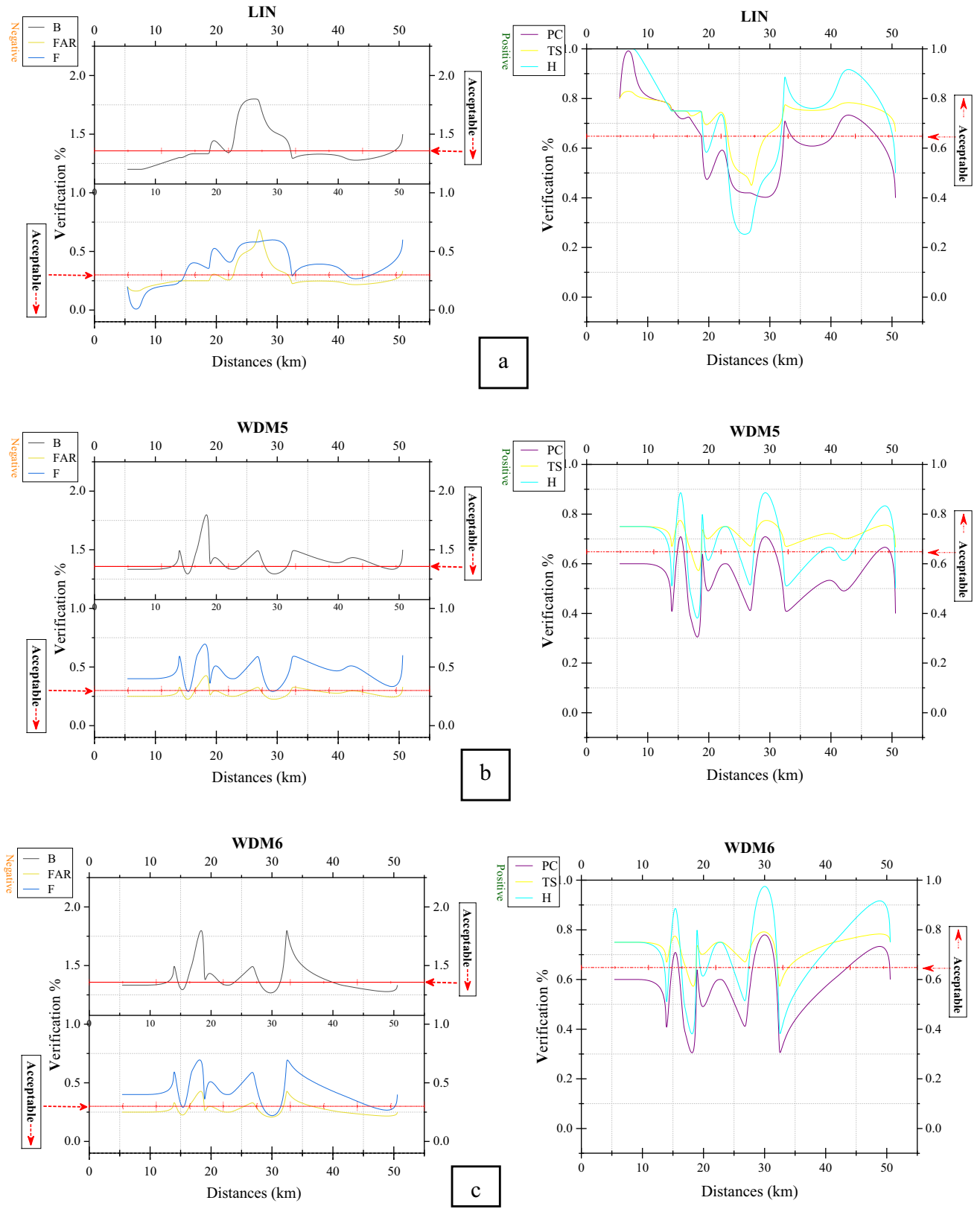


**Fig. 4** The negative and positive verification criteria related to the six WRF schemes based on the several distances from the synoptic station

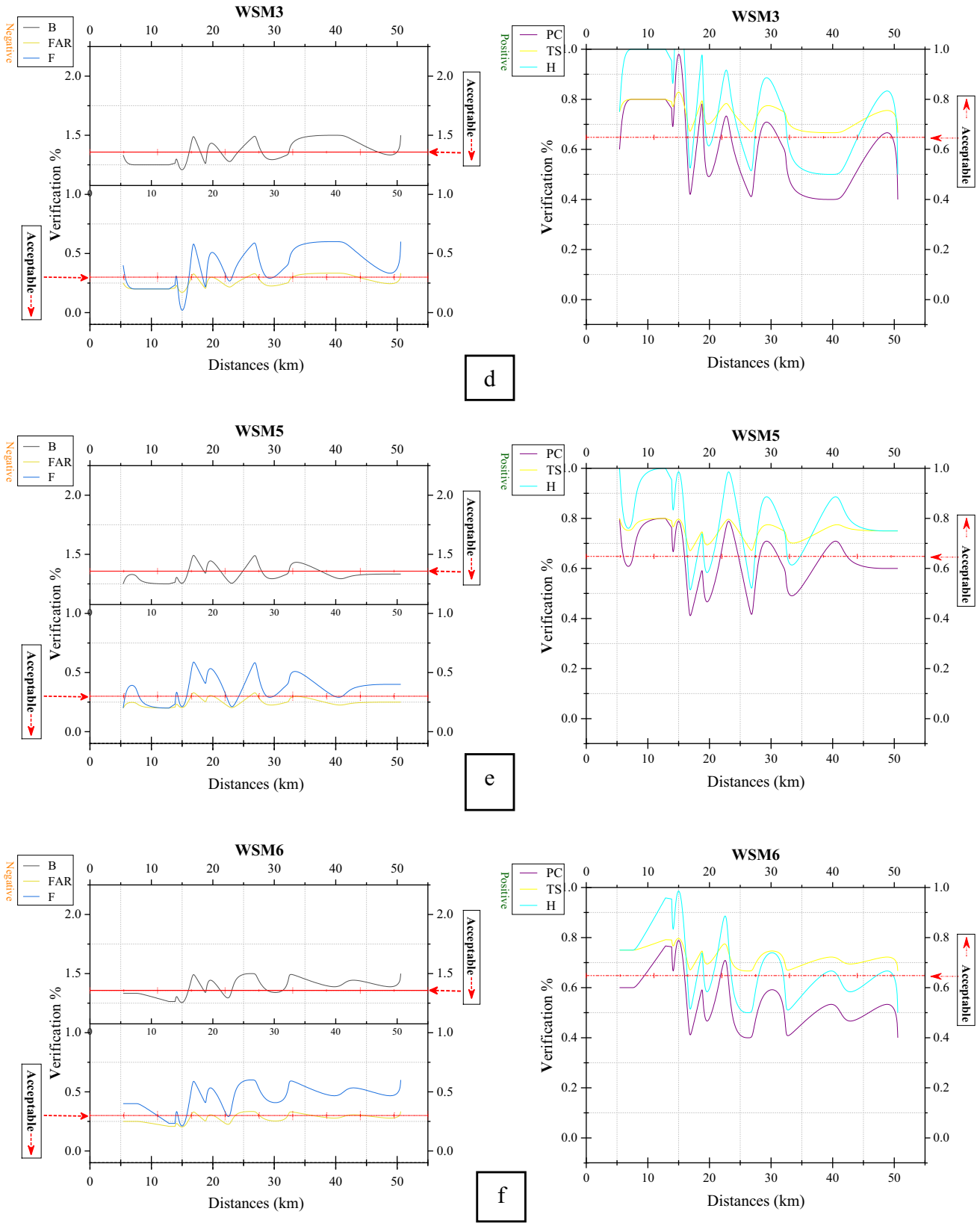


**Fig. 4** (continued)

synoptic station. Accordingly, Figs. 4a, 4b, 4c, 4d, 4e, and 4f are associated with the schemes including Lin, WDM5, WDM6, WSM3, WSM5, and WSM6, respectively. A negative verification criterion (B, FAR, and F) on the left and a positive verification criterion (PC, TS, and H) on the right of the figure have been calculated for each of these schemes in the several distances from the synoptic observational station. According to these figures, for the positive criteria (PC, TS, and H), the acceptable interval was between 0.65 and 1.00%. In other words, the closer the values are to 1.00%, the better the scheme works for each generated raingauge point. Conversely, for the negative criteria of FAR and F, the closer the values to zero, the better the scheme for each of the raingauge points (Xu et al. 2017).

Moreover, compared to the other schemes, the Lin scheme had the best performance for the distance up to 18.85 km (Fig. 4a). Accordingly, in this interval [0, 18.85], the values of the positive criteria ranged from 0.65 to 1.00%, while the values of the negative criteria were lowest between 0.00 and 1.30%. Also, as it is shown in Figs. 4b and 4c, WDM5 and WDM6 schemes had a lower performance at different distances of raingauge networks. Obviously, in these schemes, the values of positivism verification quantities were 0.65 to 0.85, whereas the negative positivism quantities were 1 and 1.75. In the study, the WSM3 scheme was identified with better accuracy and performance for raingauge station networks at different distances in comparison with the WSM6 scheme. As known, in this scheme, up to 15.5 km from the synoptic station, the precipitation rate for positive amounts is between 0.40 and 1, and for negative amounts between 0 and 1.5%. According to the Lin scheme, the WSM5 scheme has the best performance for forecasting rainfall over the study area. According to Fig. 4, this scheme is acceptable for positivism quantities within 0.60 and 0.80%, and for negative quantities within 0 and 1.33%, to a distance of 15.55 km.

Furthermore, this scheme is more accurate and efficient than satellite rainfall products (SRPs). Our results are consistent with Yu et al. (2020), who have identified four satellite products (raingauge bias-corrected Climate Prediction Center morphing technique (CMORPH CRT), Tropical Rainfall Measuring Mission (TRMM) 3B42V7); Rainfall Estimation from Remotely Sensed Information using Artificial Neural Network-Cloud Classification System (PERSIANN-CCS), and Integrated Multi-satellite Retrievals for Global Precipitation Measurement (IMERG)). In their study, IMERG showed a false alarm ratio (FAR) of up to 0.41% as the best SRP, and the same (FAR) in the WRF model for the Lin scheme was set to 0%. Furthermore, all SRPs underestimated the no/light events of no/light rainfall (0–1 mm day$^{-1}$) G. PERSIANN-CCS also showed poor performance with significant underestimation of precipitation class 1–2 mm per day$^{-1}$ and overestimation of precipitation class 2–5 mm per day$^{-1}$. In the event of 26/02/2020, the amount of observation rainfall was 0.4 mm, the WRF, whereas, in the Lin scheme for stationary networks has simulated their amount even with a difference of 0.02%.

For each station, the results of the TS verification shown in Table 4, as this is the best method to determine the certainty of the meteorological model in forecasting rainfall. This table presented the best scheme for each raingauge station. According to the results, the Lin scheme simulates rainfall most accurately at most raingauge stations. This scheme performs well up to a distance of 18.85 km, but beyond that, the performance is lower due to the different climates in the mountains and the lowlands.

### 3.2 Evaluation of raingauge station networks

Figures 5 a and b to 9 a and b depict the evaluation of raingauge networks resulting from the output of the WRF model according to the distance from the synoptic station and the height of each network point by interpolation methods. In other words, the figures present a comparison of rainfall in

**Table 4** The best schemes of the WRF model in each of the stations

| Row | Raingauge Stations (km) | Best scheme |
|---|---|---|
| 1 | 5.4 | Lin |
| 2 | 6 | Lin |
| 3 | 7.66 | Lin |
| 4 | 8.11 | Lin |
| 5 | 13.81 | Lin |
| 6 | 13.82 | WSM3,WSM5,WSM6 |
| 7 | 14.07 | Lin |
| 8 | 14.56 | Lin |
| 9 | 15.55 | Lin |
| 10 | 16.72 | Lin |
| 11 | 16.93 | Lin |
| 12 | 18.78 | Lin |
| 13 | 18.85 | Lin |
| 14 | 19.33 | WDM5,WDM6,WSM3 |
| 15 | 21.55 | Lin |
| 16 | 22.83 | WSM3,WSM5,WSM6 |
| 17 | 23.48 | WSM5 |
| 18 | 26.79 | – |
| 19 | 26.96 | – |
| 20 | 28.43 | WDM5,WDM6,WSM3,WSM5 |
| 21 | 31.95 | WDM6 |
| 22 | 32.42 | WSM3 |
| 23 | 32.73 | Lin |
| 24 | 41.1 | Lin |
| 25 | 41.48 | Lin |
| 26 | 50.26 | WDM5,WDM6,WSM3 |
| 27 | 50.58 | WDM6,WSM5 |

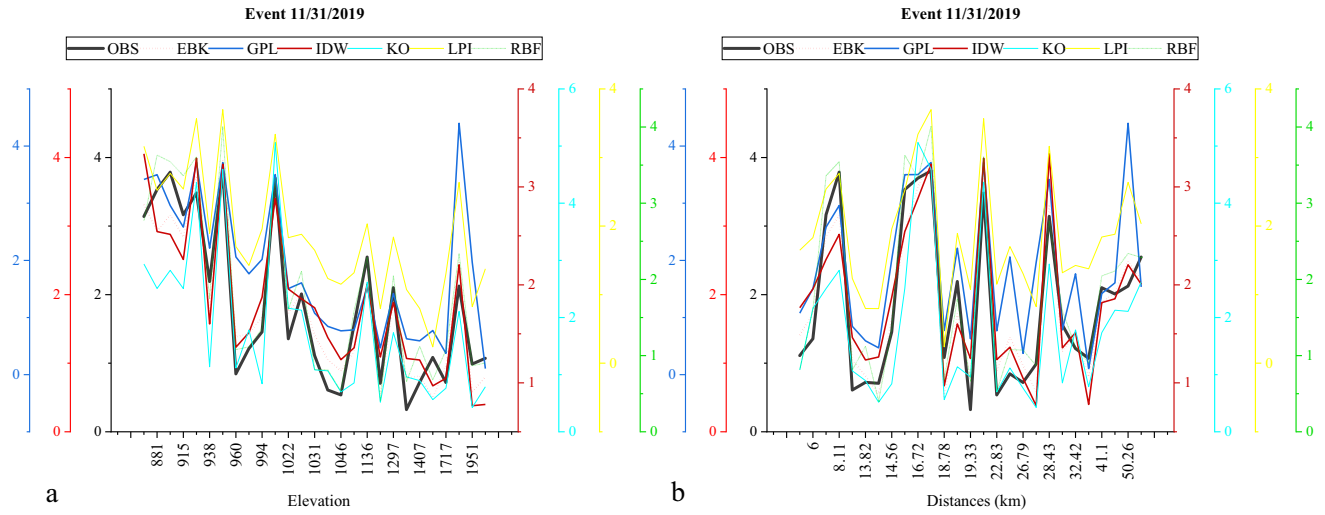


**Fig. 5** Evaluation of raingauge networks using interpolation methods in different events. **a** The rainfall values at different elevations of the catchment. **b** The rainfall values with several distances from the synoptic station

rain grids computed from the WRF model (as observation stations) and interpolation methods.

Several studies have demonstrated that the GPI method is more accurate than other geostatistical methods, as 9 out of 27 stations had a lower difference between observed and simulated data at different distances. There is an average rainfall of 0.89 mm at these points. Whereas, the difference between the observed and simulated data at different elevations of the catchment also showed that the RBF geostatistical method with 11-point stations had higher simulation accuracy. Of all methods, the IDW method has the highest error rate with 0 station points (Fig. 5a, b).

Moreover, RBF method with 19 stations had a higher accuracy, whereas the COK and IDW methods with zero stations showed the lowest accuracy by moving away from the observation station and the height of the station points at the catchment level (Fig. 6a, b). The findings of this research also showed that from the observation station up to 23.48 km, 15 stations have the highest accuracy and the distance from the observation station reduces the accuracy of rainfall. The same process works for the height of the stations, so that up to 1407 m above sea level, the accuracy of rainfall works well.

According to Fig. 7 a and b, the RBF method also had the highest accuracy of the geostatistical methods studied,

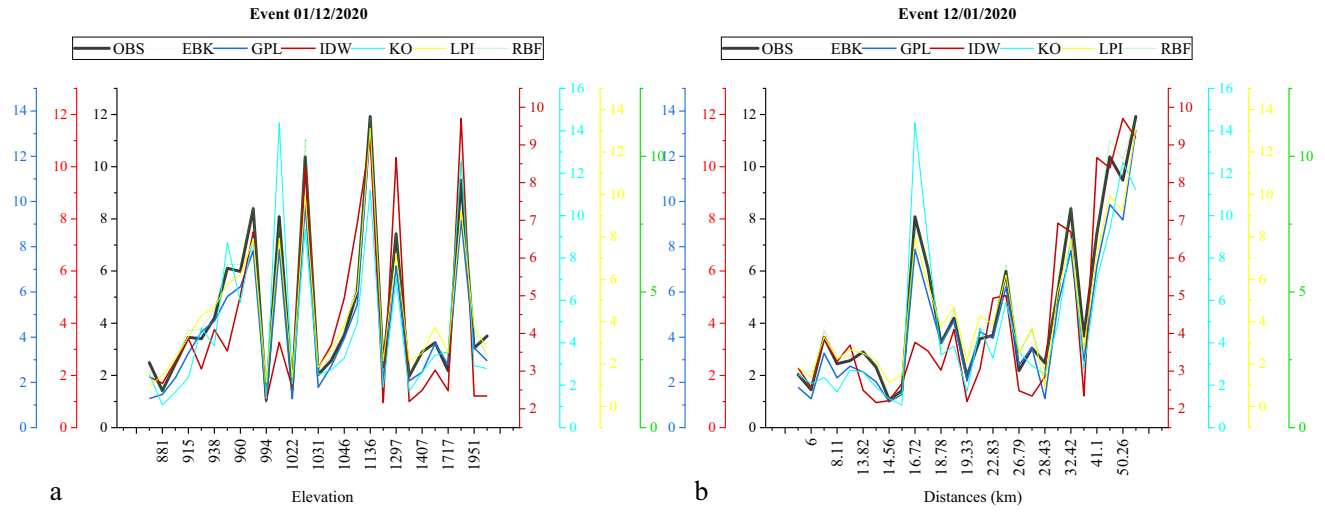


**Fig. 6** Evaluation of raingauge networks using interpolation methods in a different event. **a** The value with distance from the synoptic station. **b** The amount of rainfall at different heights of the catchment

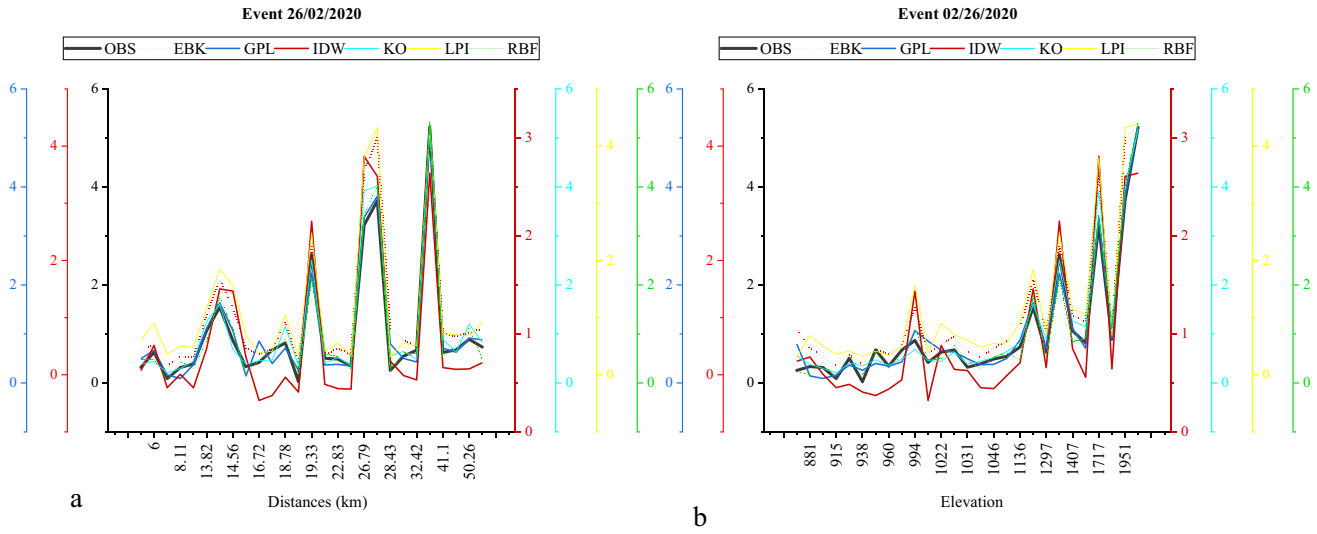


**Fig. 7** Evaluation of raingauge networks using interpolation methods in different events. **a** The value with distance from the synoptic station. **b** The amount of rainfall at different heights of the catchment

so that 8 stations had the lowest rainfall difference with the observation station in the study area. It was also found that the EBK and IDW methods with 3 stations had the lowest accuracy. In addition, the results show that the RBF method is accurate up to 992 m from stationary points, but with increasing altitude, it becomes less accurate. There was the greatest accuracy with the RBF method with 16 stations, while the lowest accuracy was associated with IDW and EBK methods with 1 point (Fig. 8a, b). These findings also showed that this method can accurately forecast rainfall amounts up to 23.48 km away from the observation station.

The average precipitation in these areas is 0.11 mm, which is simulated to be 0.90 mm at a greater distance from this station. Regarding the height of network points, it was also found that up to 1407 m, 12 points have the lowest rainfall difference from the observation station. The amount of rainfall increases by 1 mm with enhancing altitude from 1407 m.

Figure 9 a and b showed that the RBF method with 20-point stations has the highest accuracy. Whereas, other methods have the weakest accuracy with one station point, except for the LPI method, which has only 3 station points. The results of the distance from the observation station

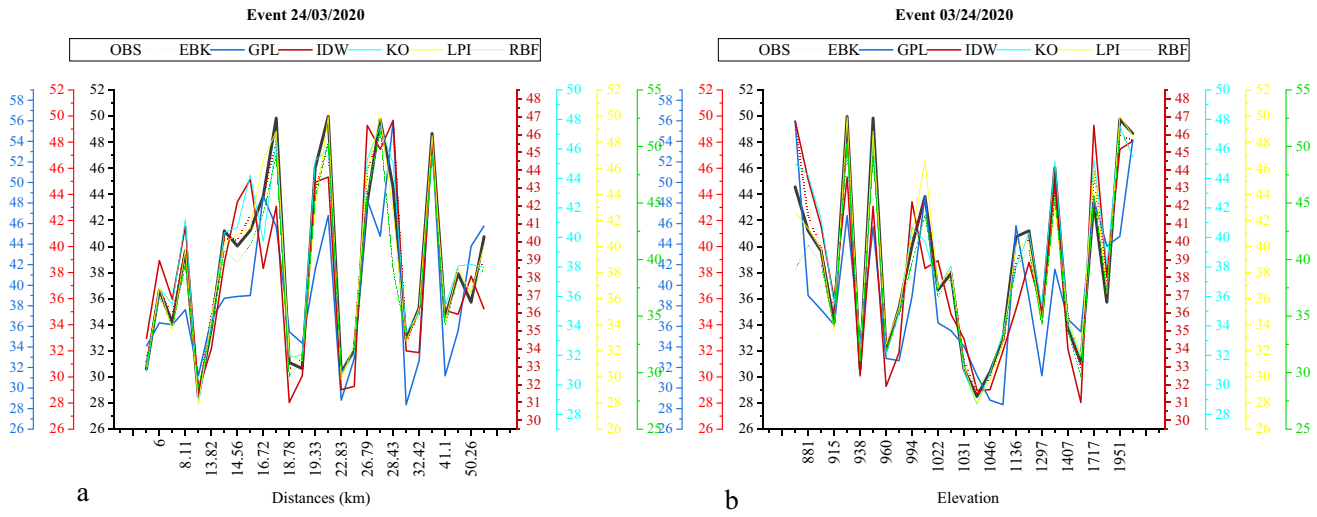


**Fig. 8** Evaluation of raingauge networks using interpolation methods in different events. **a** The value with distance from the synoptic station. **b** The amount of rainfall at different heights of the catchment

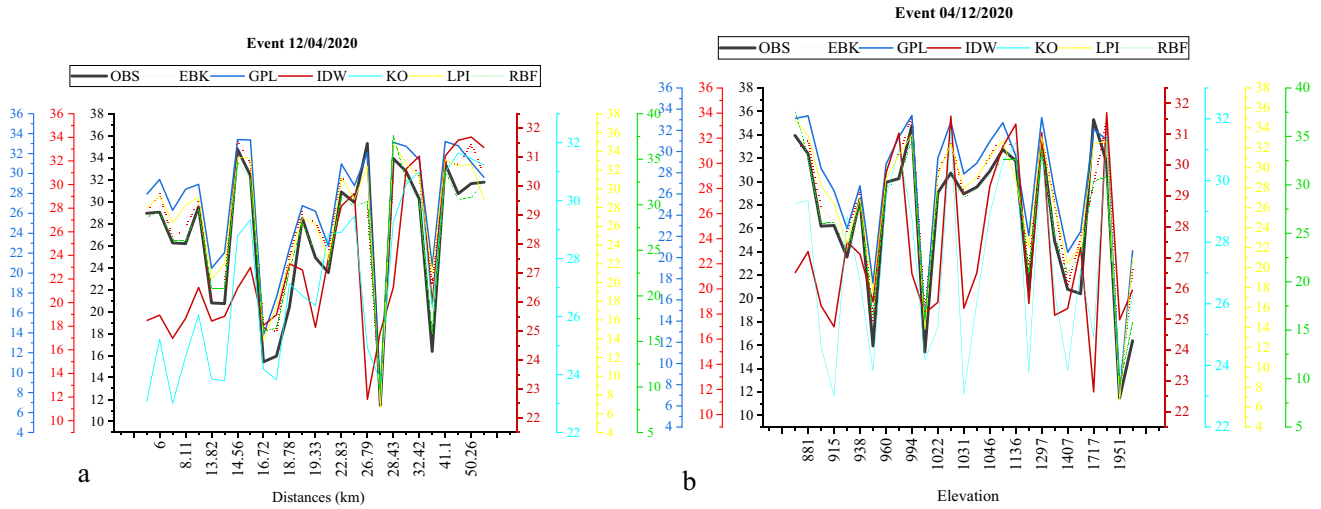


**Fig. 9** Evaluation of raingauge networks using interpolation methods in different events. **a** The value with distance from the synoptic station. **b** The amount of rainfall at different heights of the catchment

also showed that all distances had the lowest rainfall difference with an average of 0.001 mm, except for the distances from 26 to 31 km with 4 points and 50 km and more with 2 points. Based on the amount of simulation, up to the height of 1407 m, 19 points have the highest accuracy, indicating an average rainfall difference of 0.028 mm at these altitudes.

### 3.3 Measuring the accuracy of interpolation methods

Six criteria have been used to evaluate the accuracy of interpolation methods in rainfall estimation. The value of interpolation methods for accurate measurement in estimating the amount of precipitation in the network of rainfall stations at the catchment level for 27 points was illustrated in Fig. 10. Accordingly, the RBF method has higher accuracy and efficiency than other interpolation methods with the highest $R^2$ (98.04%) in all events except for 03/24/2020. In this case, the LPI method had the best efficiency and accuracy, with an $R^2$ of 98.5%. There was a value of 99% for the events of 01/12/2020 and 02/26/2020, each representing 17% of the interpolation methods. The higher the percentage and the higher the level of classification in coefficient of determination methods show the high efficiency and accuracy of interpolation methods in estimating rainfall at the network level.

As for accuracy measurement, it is clear that the lower the percentage of errors, the lower the level of classification. In other words, they illustrate the model's high efficiency and accuracy in estimating rainfall at station networks. Furthermore, the results of the study showed that the smaller the size and error of methods other than the $R^2$ method, the higher and more acceptable the evaluation and efficiency of interpolation methods.

Our results revealed that RBF provided a more accurate estimation of rainfall amounts for the network of rainfall stations than geostatistical and deterministic interpolation methods. These findings are consistent with the results of Tsintikidis et al. (2002) due to the existence of a semi-exponential function with a spatial distance between stations. Furthermore, it was found that combining these methods, can be used for small catchments with observation stations at 5.6 km. It is also possible to obtain acceptable results with a distance of 5.6 to 18 km from the stations. This is in contrast with the results of (Lee et al. 2018), Tian et al. (2018), and Ayanwale and Alabi (2019), who used satellites and radars to estimate the amount of rainfall for large catchments if this research has been used for small and urban catchments. Regarding the contribution of altitude, our results showed that of the 27 stations of the raingauge network, 22 stations have good accuracy and efficiency in estimating rainfall with the observation stations. Moreover, this model performed better than the research of Xu et al. (2017) with different altitude points. Accordingly, they identified that TRMM and GPM have False Alarm Ratios (FAR) for altitudes less than 3,000 m that are 0.38% and 0.27%, respectively, while our research had a False Alarm Ratio of 0% (Fig. 11). This figure represented the output of the best interpolation method for the study. According to this figure, the spatial distribution of the simulated rainfall values for each event has been shown in the right and the spatial distribution of the forecasted values has been represented on the left, based on the RBF method. Investigation of the findings shows that the rainfall amount predicted by the method has very little difference from the simulated amount. In fact, there is so little difference between the Sabzevar synoptic station and most of the output points of the meteorological model. Also, the investigation of the topographic conditions and the distance from the synoptic station shows that with increasing the

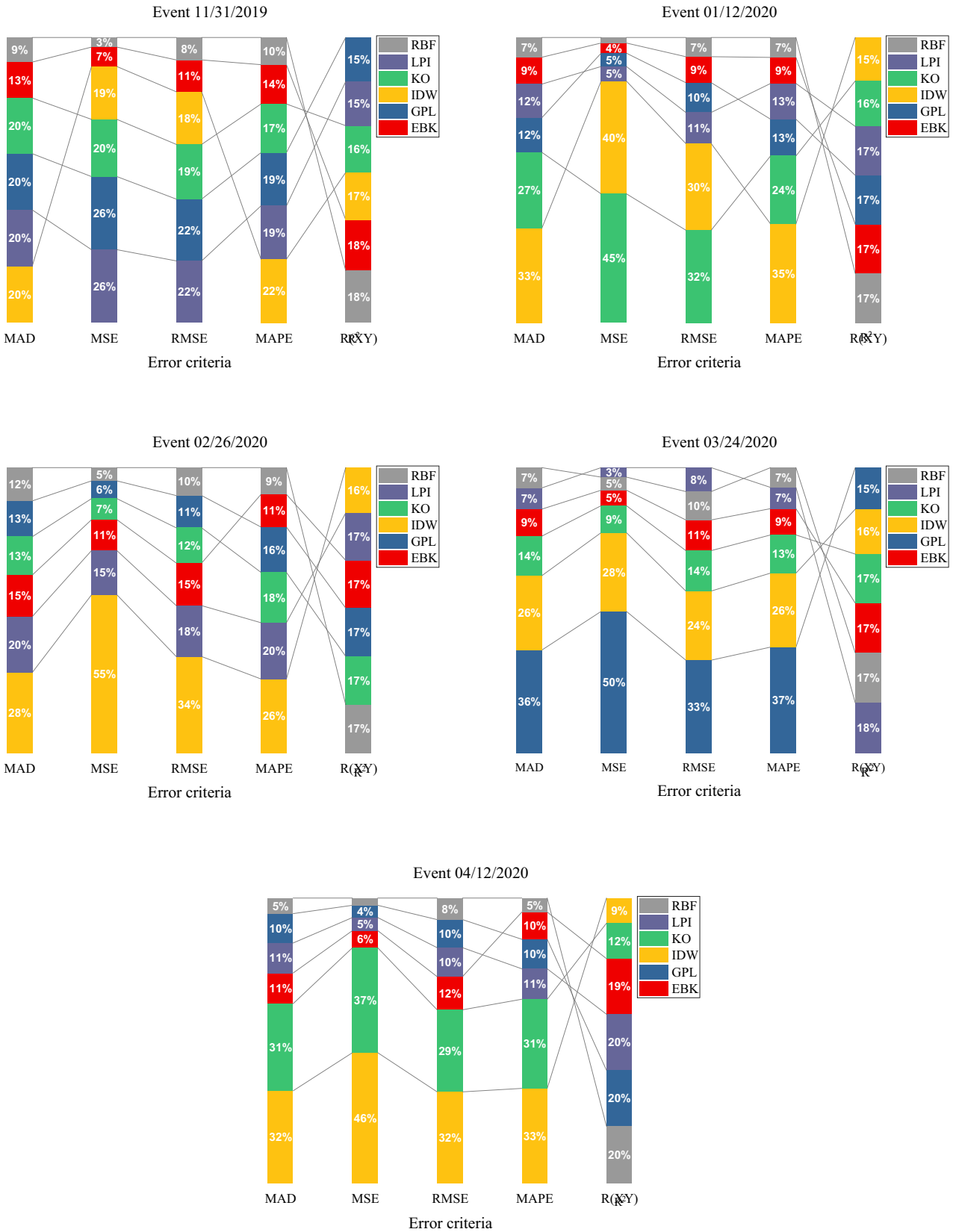


**Fig. 10** Measuring the accuracy of different interpolation methods

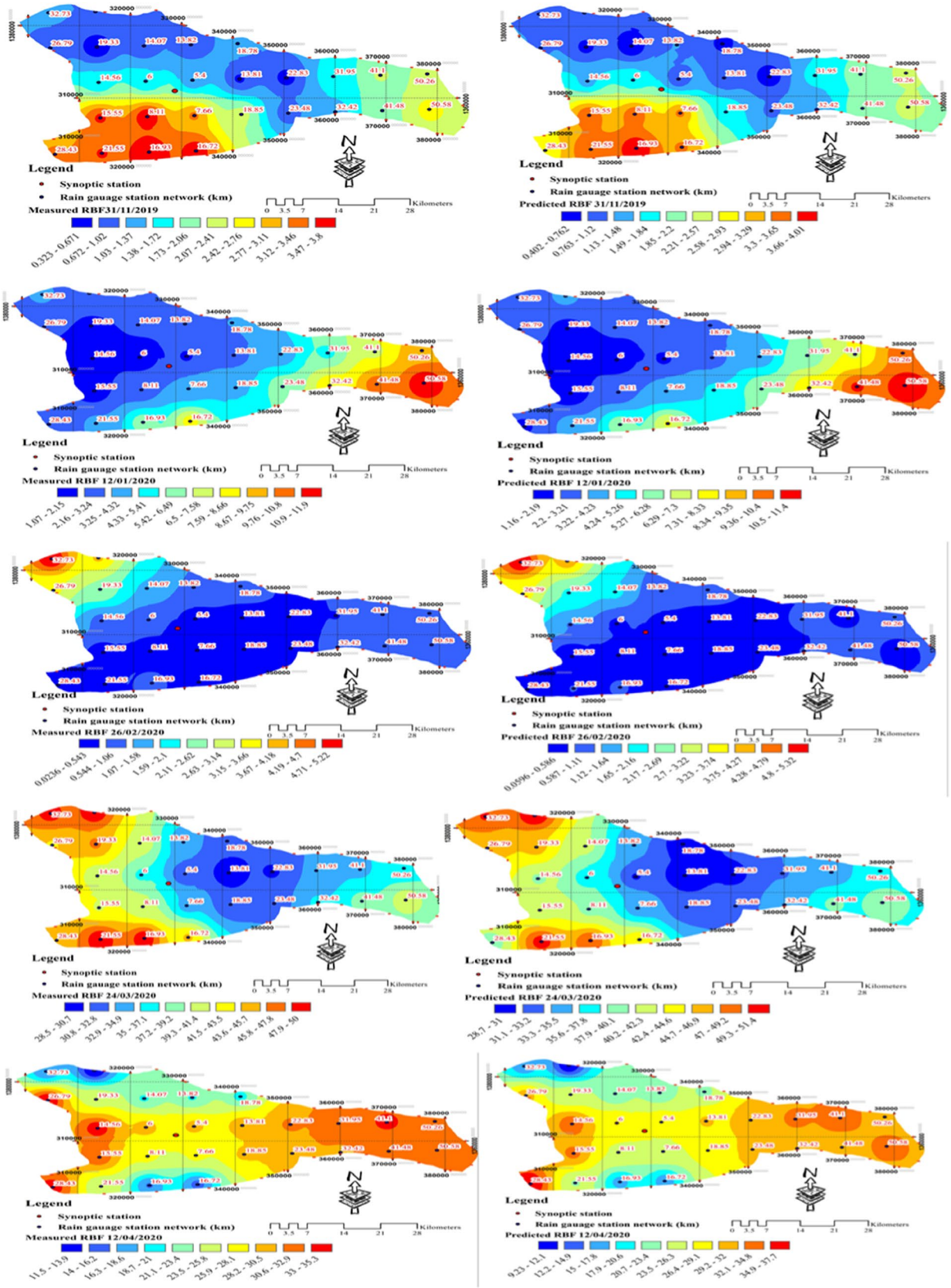


**Fig. 11** The output of the best interpolation method in different events of the study area

distance from the synoptic station, the rainfall amount changes increased. This difference shows the accuracy of the proposed method in forecasted results associated with the geographical location of the stations. Checking the height of the output stations of the meteorological model with the Sabzevar synoptic station indicates that the difference in rainfall between the Sabzevar synoptic station (height 972 m above sea level) and a station above 2000 m (model output) is large. This difference is greater with the points with a higher altitude (especially the northern areas).

According to the findings, the meteorological model and the interpolation method have acceptable accuracy in estimating the rainfall for the study area concerning the location and geographical conditions. This combination of the WRF numerical dynamic model and the spatial analysis-based interpolation method can calculate rainfall amount along with the raingauge stations network for points without stations within the catchment.

Economically, the optimal location of raingauge stations is important to better forecast the precipitation and the relevant intensity changes for effective urban catchment management. If the number of stations and the related optimal distribution is determined for the urban catchments, the cost of designing and implementing the ground stations will be decreased, significantly. Therefore, in this research, the spatial design of the raingauge stations network for the points without stations using the desirable and reliable meteorological model along with the spatial analysis-based methods and taking into account the conditions and location of the region including the rainfall, height and distance of stations, has been proposed. The advantage of this method, is the forecast of precipitation and the possibility of calculating other weather parameters for these spatial points along with ground stations.

## 4 Conclusions

Optimal station locations are necessary to determine rainfall amounts and changes in rainfall intensity during heavy rains, economically. This means that increasing sampling density will lead to better estimations of average rainfall. However, the number of stations and distribution should be selected based on the favorable conditions of the region, which is not cost-effective considering the establishment of the station and personnel costs. Therefore, this study estimated rainfall and designed rainforest networks using the WRF model and interpolation methods. Based on the results of rainfall events in the Sabzevar urban catchment, the microphysical Lin scheme was found to be more efficient and accurate. Thus, for three out of five rainfall events, this scheme showed a much smaller rainfall difference, simulates and scales precipitation more appropriately, with a smaller precipitation difference both at the observation station level and in the 27 rain grids resulting from the WRF model output.

This scheme has the best performance compared to other distances up to 18.85 km from the raingauge. At this stationary distance, the value of positive verification quantities ranges from 0.65 to 1%, and the negative verification quantities range minimally between 0 and 1.30%. Based on the results of the interpolation methods, the RBF method with 19 stations and in some cases 26 stations has an acceptable accuracy with the distance from the observation station and the height of the points at the catchment level. Moreover, the distance from the observation station reduced the level of certainty in the model. Similarly, the amount of model certainty works well up to 1407 m above sea level, where the model performance will decrease as the height value increases. Additionally, by comparing the WRF model schemes, the best schemes for the region can be identified that can be used to forecast rainfall for the next 24 h. In other words, this combination allows precipitation intensity to be determined at locations without stations and locations with existing stations, allowing their data to be used in hydrologic models. This raises awareness before flooding and flood points occur in urban areas allowing officials and managers working in the water resources field can prevent potential damage. Overall, it can be concluded that the WRF model use for large catchments is reasonable because of the acceptable output of this model for urban and small areas.

**Author contribution** All authors contributed to the study's conception and design. Material preparation, data collection, and analysis were performed by M Karami, R Javidi Sabaghiain, and R Sarvestan. The first draft of the manuscript was written by R Sarvestan and all authors commented on previous versions of the manuscript. All authors read and approved the final manuscript.

**Funding** The authors did not receive support from any organization for the submitted work.

**Data availability** Not applicable.

**Code availability** Not applicable.

## Declarations

**Competing interests** The authors declare no competing interests.

**Ethics approval** Not applicable.

**Consent to participate** Not applicable.

**Consent for publication** All authors consent to the article's publication after acceptance.

**Conflict of interest** The authors declare no competing interests.

## References


Amirahmadi A, Behniafar A, Ebrihimi M (2012) Microzonation of flood risk in Sabzevar suburb with the aim of sustainable urban development. Environ Based Territorial Plan 16:17–32

Ashraf M, Loftis JC, Hubbard KG (1997) Application of geostatistics to evaluate partial weather station networks. Agric for Meteorol 84:255–271

Atiqul IM (2018) Statistical comparison of satellite-retrieved precipitation products with raingauge observations over Bangladesh. Int J Remote Sens 39:2906–2936

Ayanwale OA, Alabi O (2019) Ground validation of GPM IMERG and TRMM 3B42V7 rainfall products over Nigerian Lightning. J Geophys Res Atmos 122(2):910–924

Bayat B, Hosseini K, Nasseri M, Karami H (2019) Challenge of rainfall network design considering spatial versus spatiotemporal variations. J Hydrol 574:990–1002

Cao Q, Jiang B, Shen X, Lin W, Chen J (2021) Microphysics effects of anthropogenic aerosols on urban heavy precipitation over the Pearl River Delta, China. Atmos Res 253:105–478

Cecinati F, Moreno-Ródenas AM, Rico-Ramirez MA, Ten Veldhuis M-C, Langeveld JG (2018) Considering raingauge uncertainty using kriging for uncertain data. Atmosphere 9:446

Cheng K-S, Lin Y-C, Liou J-J (2008) Rain-gauge network evaluation and augmentation using geostatistics. Hydrological Processes: an International Journal 22:2554–2564

de Bodas Terassi PM, de Oliveira-Junior JF, de Gois G, Júnior ACO, Sobral BS, Biffi VH R, Vijith H (2020) Rainfall and erosivity in the municipality of Rio de Janeiro-Brazil. Urban Clim 33:100637

El Afandi G, Morsy M (2020) Developing an early warning system for flash flood in Egypt: case study Sinai Peninsula. In: Negm A (ed) Flash floods in Egypt. Advances in Science, Technology & Innovation. Springer, Cham, pp 45–60. https://doi.org/10.1007/978-3-030-29635-3_4

Guo J, Lei H, Chen D, Yang J (2019) Evaluation of the WDM6 scheme in the simulation of number concentrations and drop size distributions of warm-rain hydrometeors: comparisons with the observations and other schemes. Atmos Ocean Sci Lett 12(6):458–466

Handmer J, Honda Y, Kundzewicz ZW, Arnell N, Benito G, Hatfield J, Mohamed IF, Yamano H (2012) Managing the risks of extreme events and disasters to advance climate change adaptation. Special report of the intergovernmental panel on climate change, 9781107025066:231–290

Hong S-Y, Lim J-OJ (2006) The WRF single-moment 6-class microphysics scheme (WSM6). Asia-Pacific Journal of Atmospheric Sciences 42(2):129–151

Hong S-Y, Dudhia J, Chen S-H (2004) A revised approach to ice microphysical processes for the bulk parameterization of clouds and precipitation. Mon Weather Rev 132(1):103–120

Hong S-Y, Lim K-SS, Lee Y-H, Ha J-C, Kim H-W, Ham S-J, Dudhia J (2010) Evaluation of the WRF double-moment 6-class microphysics scheme for precipitating convection. Adv Meteorol 1–10. https://doi.org/10.1155/2010/707253

Hu L, Nikolopoulos EI, Marra F, Morin E, Marani M, Anagnostou EN (2020) Evaluation of MEVD-based precipitation frequency analyses from quasi-global precipitation datasets against dense raingauge networks. J Hydrol 590:125564

Huang J, Fatichi S, Mascaro G, Manoli G, Peleg N (2022) Intensification of sub-daily rainfall extremes in a low-rise urban area. Urban Climate 42:101124

Jones JW, Hoogenboom G, Porter CH, Boote KJ, Batchelor WD, Hunt LA, Wilkens PW, Singh U, Gijsman AJ, Ritchie JT (2003) The DSSAT cropping system model. Eur J Agron 18:235–265

Kedem B, Chiu LS, Karni Z (1990) An analysis of the threshold method for measuring area-average rainfall. J Appl Meteorol Climatol 29:3–20

Khansalari S, Ranjbar-Saadatabadi A, Fazel-Rastgar F, Raziei T (2021) Synoptic and dynamic analysis of a flash flood-inducing heavy rainfall event in arid and semi-arid central-northern Iran and its simulation using the WRF model. Dyn Atmos Oceans 93:101198

Lee J, Kim S, Hwandon J (2018) A study of the influence of the spatial distribution of raingauge networks on areal average rainfall calculation. Water 10:1635

Mahala BK, Mohanty PK, Xalxo KL, Routray A, Misra SK (2021) Impact of WRF Parameterization Schemes on Track and Intensity of Extremely Severe Cyclonic Storm Fani. Pure Appl Geophys 178(1):245–268

Meteorological Organization (2019) Precipitation, temperature, and evapotranspiration data. Iranian Meteorological Organization of Iran, pp 48–62

Morin E, Krajewski WF, Goodrich DC, Gao X, Sorooshian S (2003) Estimating rainfall intensities from weather radar data: the scale-dependency problem. J Hydrometeorol 4:782–797

Morin E, Maddox RA, Goodrich DC, Sorooshian S (2005) Radar Z-R relationship for summer monsoon storms in Arizona. Weather Forecast 20:672–679

Mu Ye, Biggs T, Samuel S, Shen P (2021) Satellite-based precipitation estimates using a dense rain-gauge network over the Southwestern Brazilian Amazon: Implication for identifying trends in dry season rainfall. Atmos Res 261:10–36. https://doi.org/10.1016/j.atmosres.2021.105741

Naing SM (2021) Sensitivity Analysis of Heavy Rainfall Events on Physical Parameterization Configurations Using WRF-ARW Model over Myanmar, pp 1–125

O'Gorman PA (2015) Precipitation extremes under climate change. Current Climate Change Reports 1:49–59

Rossi M, Kirschbaum D, Valigi D, Mondini AC, Guzzetti F (2017) Comparison of satellite rainfall estimates and raingauge measurements in Italy, and impact on landslide modeling. Climate 5:90

Shafiei M, Ghahraman B, Saghafian B, Pande S, Gharari S, Davary K (2014) Assessment of Raingauge networks using a probabilistic GIS based approach. Hydrol Res 45:551–562

Shimizu K (1993) A bivariate mixed lognormal distribution with an analysis of rainfall data. J Appl Meteorol Climatol 32:161–171

Shirali E, Shahbazi AN, Fathian H, Zohrabi N, Hassan EM (2020) Evaluation of WRF and artificial intelligence models in short-term rainfall, temperature and flood forecast (case study). J Earth Syst Sci 129:1–16

Smith JA, Seo DJ, Baeck ML, Hudlow MD (1996) An intercomparison study of NEXRAD precipitation estimates. Water Resour Res 32:2035–2045

Steduto P, Hsiao TC, Raes D, Fereres E (2009) 'AquaCrop—The FAO crop model to simulate yield response to water: I Concepts and Underlying Principles. Agronomy J 101:426–437

Tekleyohannes M, GrumG B, Niguse A, Bizuneh A (2021) Optimization of rain gauge network using multi-criteria decision analysis and Entropy approaches case of Tekeze River basin, northwestern Ethiopia. Theor Appl Climatol 145(1–2):1–16. https://doi.org/10.1007/s00704-021-03604-1

Tian F, Hou S, Yang L, Hongchang Hu, Hou A (2018) How does the evaluation of the GPM IMERG rainfall product depend on gauge density and rainfall intensity? J Hydrometeorol 19:339–349

Tsintikidis D, Georgakakos KP, Sperfslage JA, Smith DE, Carpenter TM (2002) Precipitation uncertainty and raingauge network design within Folsom Lake watershed. J Hydrol Eng 7:175–184

Villarini G, Pradeep V, Mandapa, Witold F, Krajewski, Robert J (2008) Rainfall and sampling uncertainties: a rain gauge perspective. J Geophys Res Atmos 113:1–12. https://doi.org/10.1029/2007JD009214

Volkmann T, Steve W, Hoshin V, Peter A (2010) Multicriteria design of rain gauge networks for flash flood prediction in semiarid catchments with complex terrain. Water Resour Res 46:1–16. https://doi.org/10.1029/2010WR009145

Wang J, Huang B, Huang A, Goldberg MD (2011) Parallel computation of the weather research and forecast (WRF) WDM5 cloud microphysics on a many-core gpu. Paper presented at the 2011 IEEE 17th International Conference on Parallel and Distributed Systems, pp 1032–1037

Xavier AC, King CW, Scanlon BR (2016) Daily gridded meteorological variables in Brazil (1980–2013). Int J Climatol 36:2644–2659

Xu H, Chong-Yu Xu, Sælthun NR, Youpeng Xu, Zhou B, Chen H (2015) Entropy theory based multi-criteria resampling of raingauge networks for hydrological modelling–a case study of humid area in southern China. J Hydrol 525:138–151

Xu R, Tian F, Yang L, Hongchang Hu, Hui Lu, Hou A (2017) Ground validation of GPM IMERG and TRMM 3B42V7 rainfall products over southern Tibetan Plateau based on a high-density raingauge network. J Geophys Res: Atmos 122:910–924

Yoo C, Jung K, Lee J (2008) Evaluation of raingauge network using Entropy theory: comparison of mixed and continuous distribution function applications. J Hydrol Eng 13:226–235

Young CB, Nelson BR, Allen Bradley A, Smith JA, Peters-Lidard CD, Kruger A, Baeck ML (1999) An evaluation of NEXRAD precipitation estimates in complex terrain. J Geophys Res: Atmos 104:19691–19703

Yu L, Ma L, Li H, Zhang Y, Kong F, Yang Y (2020) Assessment of high-resolution satellite rainfall products over a gradually elevating mountainous terrain based on a high-density raingauge network. Int J Remote Sens 41:5620–5644